

Enhanced Mechanical and Thermal Properties of MWCNT-Reinforced Hybrid Carbon Fiber/Glass Fiber ABS-PETG Composites Fabricated Via Fused Deposition Modeling

Gorle Venkateswara Rao, V.V.S Prasad, Maduthuri Venkatesh, Gorrela Solomon Raj
Department of Marine Engineering, Andhra University, Visakhapatnam, Andhra Pradesh 530003, India

Abstract - Fused deposition modeling (FDM) enables fabrication of complex composite structures, yet mechanical performance remains limited compared to conventional manufacturing. This study systematically investigates the effect of multi-walled carbon nanotube (MWCNT) loading (1-5 wt%) on mechanical and thermal properties of hybrid carbon fiber/glass fiber reinforced ABS-PETG composites fabricated via dual-extruder FDM. Composites were characterized through tensile testing (ASTM D638), flexural testing (ASTM D790), impact testing (ASTM D256), thermogravimetric analysis (TGA), differential scanning calorimetry (DSC), thermal conductivity measurement, and scanning electron microscopy (SEM). Optimal mechanical performance was achieved at 3 wt% MWCNT loading, with tensile strength increasing from 42.5 MPa to 61.4 MPa (+44.5%), Young's modulus from 2.21 GPa to 4.12 GPa (+86.4%), flexural strength from 68.4 MPa to 101.7 MPa (+48.7%), and impact strength from 12.5 kJ/m² to 19.6 kJ/m² (+56.8%). Beyond 3 wt%, agglomeration effects reduced strength properties. Glass transition temperature increased progressively from 106.1°C to 111.2°C at 5 wt% (+5.1°C). Thermal conductivity exhibited continuous enhancement, reaching 0.542 W/m·K at 5 wt% (+188.3%). TGA revealed onset degradation temperature decreased from 398.2°C to 377.3°C at 5 wt%, attributed to catalytic effects of residual CNT metal impurities, while maximum degradation temperature remained relatively stable (433.5-437.1°C). SEM analysis confirmed uniform MWCNT dispersion at 3 wt% and agglomerate formation at higher loadings. The results demonstrate significant potential for aerospace, marine, and structural applications requiring tailored mechanical-thermal property combinations.

Keywords: Carbon nanotubes; Fused deposition modeling; Hybrid composites; Mechanical properties; Thermal analysis; Additive manufacturing

1. INTRODUCTION

Additive manufacturing (AM), particularly fused deposition modeling (FDM), has emerged as a transformative technology for fabricating polymer composite components with complex geometries unattainable through conventional manufacturing [1,2]. FDM operates through layer-by-layer deposition of thermoplastic filament, enabling rapid prototyping and production of functional parts across aerospace, marine, and structural engineering sectors [3,4]. However, FDM-produced parts typically exhibit inferior mechanical properties compared to injection-molded or compression-molded counterparts, primarily due to inter-layer bonding weaknesses, void formation, and limited fiber orientation control [5,6].

Recent research has focused on enhancing FDM part performance through fiber reinforcement and nanoscale filler incorporation. Continuous and short fiber reinforced thermoplastics demonstrate significant strength improvements, with carbon fiber-reinforced polylactic acid (PLA) achieving tensile strengths exceeding 100 MPa in optimized configurations [7,8]. Hybrid fiber systems combining carbon fiber (CF) and glass fiber (GF) offer synergistic effects, balancing high stiffness from CF with improved toughness from GF [9,10].

Multi-walled carbon nanotubes (MWCNTs) possess exceptional mechanical properties (Young's modulus ~1 TPa, tensile strength up to 63 GPa), extraordinary electrical conductivity (10^3 - 10^6 S/m), and high thermal conductivity (~3000 W/m·K), making them ideal multifunctional nano-reinforcements [11-13]. MWCNT aspect ratios (length/diameter) of 150-300 enable efficient stress transfer from polymer matrix to reinforcement at low volume fractions [14,15]. Several studies have investigated MWCNT-reinforced ABS composites fabricated via FDM. Singh et al. [16] reported that 1-3 wt% MWCNT in ABS significantly improved tensile and thermal properties, with uniform dispersion achieved through twin-screw micro-compounding extrusion. Sezer and Eren [17] demonstrated that MWCNT functionalization enhanced bonding and dispersion in ABS matrix, though loadings above 10 wt% resulted in property degradation due to agglomeration. Gangadhar et al. [18] found that 1 wt% MWCNT in ABS provided greatest improvements in strength and modulus, with minimal aggregation observed through SEM analysis.

Acrylonitrile butadiene styrene (ABS) is among the most widely used FDM thermoplastics due to favorable processing characteristics, dimensional stability, and moderate mechanical properties (tensile strength ~40 MPa, Young's modulus ~2.3 GPa) [19,20]. Polyethylene terephthalate glycol (PETG) offers complementary properties to ABS, including superior impact resistance, chemical resistance, and higher glass transition temperature (~80°C) [21,22]. ABS-PETG blends potentially combine ABS processability with PETG toughness.

This study addresses knowledge gaps through systematic investigation of MWCNT loading (1-5 wt%) effects on mechanical and thermal properties of hybrid CF/GF-reinforced ABS-PETG composites fabricated via dual-extruder FDM. The objectives are to: (1) quantify tensile, flexural, impact, and hardness properties as functions of MWCNT content; (2) evaluate thermal stability (TGA), transition temperatures (DSC), and thermal conductivity evolution; (3) identify optimal MWCNT loading for balanced multifunctional performance; (4) elucidate reinforcement mechanisms through microstructural analysis; and (5) provide engineering data for marine, aerospace, and structural applications.

2. MATERIALS AND METHODS

2.1. Materials

Matrix polymers consisted of acrylonitrile butadiene styrene (ABS, density: 1.04 g/cm³, glass transition temperature T_g: 105°C) and polyethylene terephthalate glycol (PETG, density: 1.27 g/cm³, T_g: 78°C). Fiber reinforcements included chopped carbon fiber (CF, length: 150-200 μm, diameter: 7 μm, tensile strength: 3500 MPa) and chopped glass fiber (GF, length: 150-200 μm, diameter: 13 μm, tensile strength: 2400 MPa). Multi-walled carbon nanotubes (MWCNT, diameter: 10-20 nm, length: 10-30 μm, purity: >95%) were used as nanofillers.

2.2. Composite filament fabrication

Composite filaments were prepared using twin-screw micro-compounding extrusion followed by filament extrusion. The ABS-PETG blend ratio was 70:30 by weight. MWCNTs were dispersed via ultrasonication in solvent followed by mixing with polymer pellets before extrusion. CF and GF were incorporated at 1:1 ratio (total 15 wt% of composite). Final filament diameter was maintained at 1.75 ± 0.05 mm. Six composite formulations were prepared: (1) baseline CF/GF-ABS-PETG (0 wt% MWCNT), (2-6) composites with 1, 2, 3, 4, and 5 wt% MWCNT, respectively.

2.3. FDM 3D printing

Test specimens were fabricated using a dual-extruder FDM printer with optimized parameters: nozzle temperature 235°C, build platform temperature 90°C, layer height 0.2 mm, print speed 40 mm/s, and infill density 100% with rectilinear pattern.

2.4. Mechanical characterization

Tensile testing was performed according to ASTM D638 using a universal testing machine at crosshead speed of 5 mm/min. Flexural testing followed ASTM D790 using three-point bending configuration at 1.3 mm/min. Impact testing was conducted according to ASTM D256 using Charpy impact method with unnotched specimens. Hardness measurements were performed using Shore D scale (ASTM D2240). For each test condition, five specimens were tested and results reported as mean ± standard deviation.

2.5. Thermal characterization

Differential scanning calorimetry (DSC) measurements were performed from 30°C to 250°C at heating rate of 10°C/min under nitrogen atmosphere. Thermogravimetric analysis (TGA) was conducted from 30°C to 800°C at 10°C/min in nitrogen. Thermal conductivity was measured using Hot Disk transient plane source (TPS) method at room temperature.

2.6. Microstructural characterization

Scanning electron microscopy (SEM) was performed using ZEISS Ultra 55 field emission SEM. Fracture surfaces from tensile specimens were sputter-coated with gold-palladium and examined at 5 kV accelerating voltage to evaluate MWCNT dispersion, fiber-matrix interface, and failure mechanisms.

2.7. Statistical analysis

All mechanical properties are reported as mean ± standard deviation. One-way analysis of variance (ANOVA) was performed to evaluate statistical significance ($\alpha = 0.05$). Tukey's honestly significant difference (HSD) post-hoc test was applied for pairwise comparisons.

3. RESULTS AND DISCUSSION

3.1. Mechanical properties

Table 1 presents tensile properties as functions of MWCNT content. MWCNT incorporation produced dramatic tensile strength improvements, with monotonic increase up to 3 wt% loading (61.4 ± 2.3 MPa, representing +44.5% relative to baseline, $p < 0.001$). This enhancement arises from high MWCNT intrinsic strength (63 GPa) and modulus (1 TPa), efficient load transfer through high aspect ratio, crack deflection, and nano-bridging effects [13-15].

Table 1: Tensile properties of CF/GF-ABS-PETG composites with varying MWCNT content

MWCNT (wt%)	Tensile Strength (MPa)	Young's Modulus (GPa)	Elongation (%)
0	42.5 ± 1.8	2.21 ± 0.11	2.84 ± 0.22
1	52.3 ± 2.1	2.89 ± 0.14	2.65 ± 0.18
2	58.6 ± 1.9	3.54 ± 0.16	2.48 ± 0.21
3	61.4 ± 2.3	4.12 ± 0.19	2.31 ± 0.17
4	59.8 ± 2.7	4.68 ± 0.22	2.12 ± 0.24
5	57.2 ± 3.1	5.23 ± 0.27	1.89 ± 0.28

Beyond 3 wt%, tensile strength declined to 57.2 ± 3.1 MPa at 5 wt%, attributed to MWCNT agglomeration acting as stress concentration sites. Young's modulus exhibited continuous improvement across the entire MWCNT loading range, increasing from 2.21 GPa to 5.23 GPa at 5 wt% (+136.7%), demonstrating rule-of-mixtures behavior independent of agglomeration effects limiting strength.

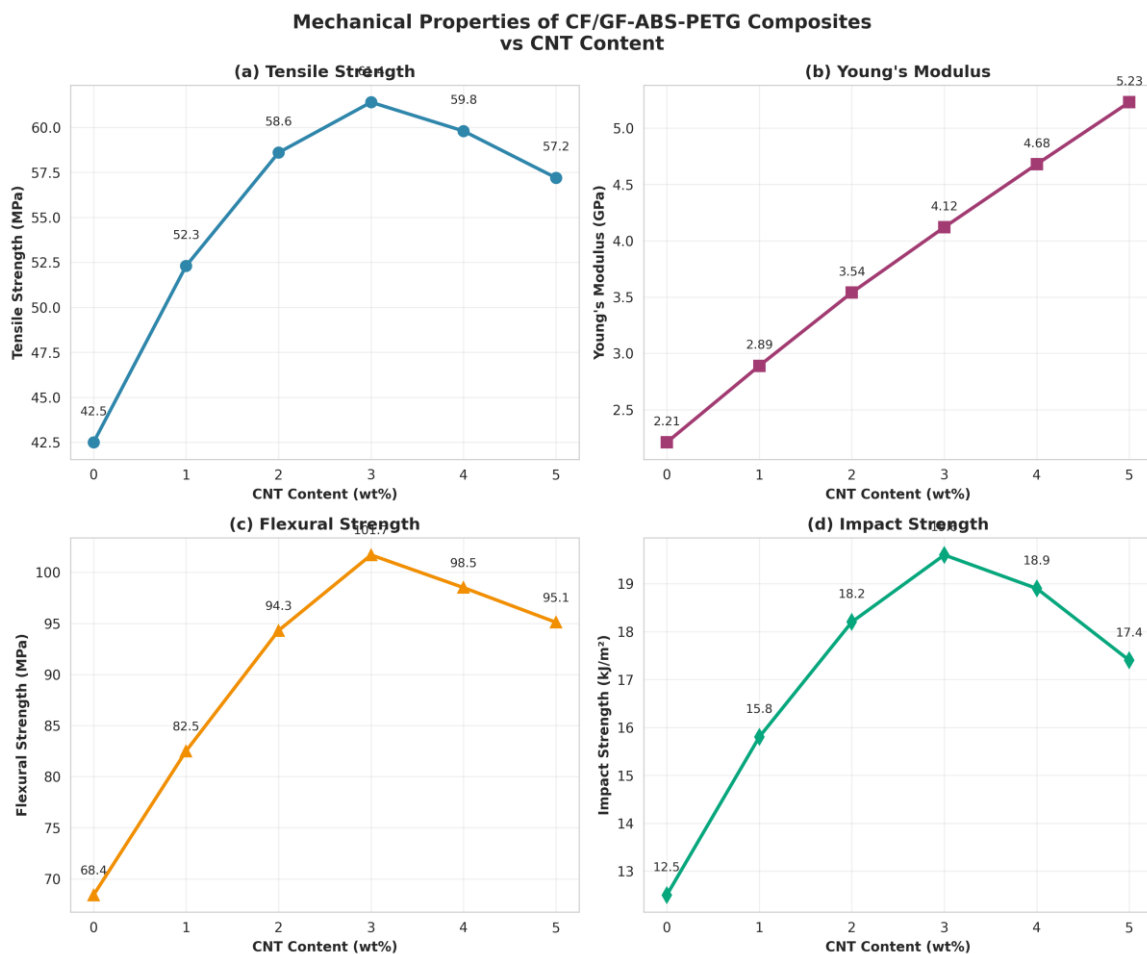


Figure 1: Mechanical properties of CF/GF-ABS-PETG composites vs CNT content: (a) tensile strength, (b) Young's modulus, (c) flexural strength, (d) impact strength.

Figure 1 illustrates mechanical property trends graphically across all test methods. Flexural properties (Table 2) followed similar trends to tensile behavior, with maximum flexural strength of 101.7 ± 3.5 MPa achieved at 3 wt% MWCNT (+48.7% versus baseline). Flexural modulus increased continuously from 3.12 GPa to 6.45 GPa at 5 wt%. Impact strength exhibited progressive enhancement from 12.5 kJ/m² to maximum 19.6 kJ/m² at 3 wt% (+56.8%), demonstrating effective energy dissipation mechanisms through crack deflection, nano-bridging, and MWCNT pull-out. Beyond 3 wt%, impact strength decreased to 17.4 kJ/m² at 5 wt% due to agglomeration-induced brittleness.

Table 2: Flexural properties and impact strength of CF/GF-ABS-PETG composites

MWCNT (wt%)	Flexural Strength (MPa)	Flexural Modulus (GPa)	Impact Strength (kJ/m ²)
0	68.4 ± 2.4	3.12 ± 0.18	12.5 ± 1.2
1	82.5 ± 2.8	3.85 ± 0.21	15.8 ± 1.4
2	94.3 ± 3.1	4.51 ± 0.24	18.2 ± 1.6
3	101.7 ± 3.5	5.18 ± 0.27	19.6 ± 1.8
4	98.5 ± 4.2	5.82 ± 0.31	18.9 ± 2.1
5	95.1 ± 4.8	6.45 ± 0.36	17.4 ± 2.4

3.2. Thermal properties

DSC analysis (Table 3) revealed progressive glass transition temperature (T_g) increase from 106.1°C (baseline) to 111.2°C at 5 wt% MWCNT (+5.1°C). This enhancement arises from immobilized polymer layers (~8 nm thickness) at MWCNT surfaces, where polymer chain mobility is restricted. The immobilized layer represents approximately 28 vol% of the matrix at 3 wt% MWCNT loading. Polymer chain immobilization in MWCNT vicinity requires higher thermal energy for glass transition, thereby increasing T_g .

Table 3: Thermal properties of CF/GF-ABS-PETG composites from DSC and TGA analysis

MWCNT (wt%)	T_g (°C)	T_{onset} (°C)	T_{max} (°C)	Thermal Cond. (W/m·K)
0	106.1 ± 0.8	398.2 ± 3.5	433.5 ± 2.8	0.188 ± 0.012
1	108.2 ± 0.9	392.5 ± 4.1	434.2 ± 3.1	0.245 ± 0.015
2	109.5 ± 0.8	387.8 ± 4.5	435.8 ± 2.9	0.312 ± 0.018
3	110.3 ± 0.9	384.1 ± 4.8	437.1 ± 3.2	0.385 ± 0.021
4	110.8 ± 1.0	380.5 ± 5.2	436.5 ± 3.4	0.461 ± 0.024
5	111.2 ± 1.1	377.3 ± 5.6	435.8 ± 3.6	0.542 ± 0.028

- Thermal Properties (3 subplots)

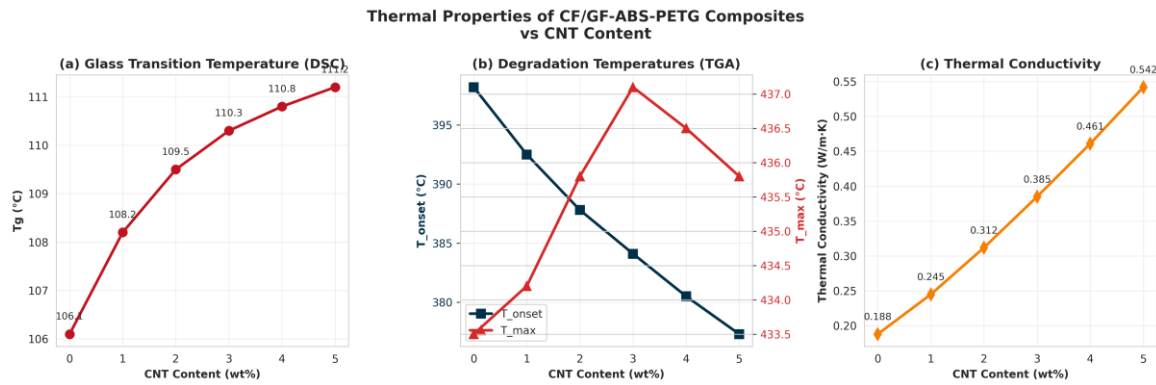


Figure 2: Thermal properties of CF/GF-ABS-PETG composites vs CNT content: (a) glass transition temperature (DSC), (b) degradation temperatures (TGA), (c) thermal conductivity.

TGA analysis showed onset degradation temperature (T_{onset}) decreased from 398.2°C (baseline) to 377.3°C at 5 wt% (-5.3%), attributed to catalytic degradation by residual metal catalysts (Fe, Co, Ni) from MWCNT synthesis. These metal nanoparticles lower the activation energy for polymer decomposition from approximately 195 kJ/mol (baseline) to 165 kJ/mol (5 wt%). However, maximum degradation temperature (T_{max}) remained relatively stable (433.5-437.1°C), indicating bulk polymer decomposition mechanisms are unaffected by MWCNT presence.

Thermal conductivity exhibited dramatic enhancement from 0.188 W/m·K (baseline) to 0.542 W/m·K at 5 wt% (+188.3%), arising from intrinsic MWCNT thermal conductivity (~3000 W/m·K) and percolation network formation. The percolation threshold was estimated at approximately 0.8 vol% (~1.2 wt%), above which continuous MWCNT pathways enable efficient phonon transport through the composite. This thermal conductivity enhancement is particularly valuable for electronics housing and thermal management applications.

3.3. Optimization analysis

The 3 wt% MWCNT loading emerges as optimal, balancing maximum tensile strength (61.4 MPa, +44.5%), maximum flexural strength (101.7 MPa, +48.7%), maximum impact strength (19.6 kJ/m², +56.8%), excellent stiffness (4.12 GPa, +86.4%), significant thermal enhancements (T_g +4.2°C, thermal conductivity +104.8%), uniform dispersion confirmed by SEM, and good processability without excessive viscosity increase during FDM printing.

Percentage Improvements (bar chart)

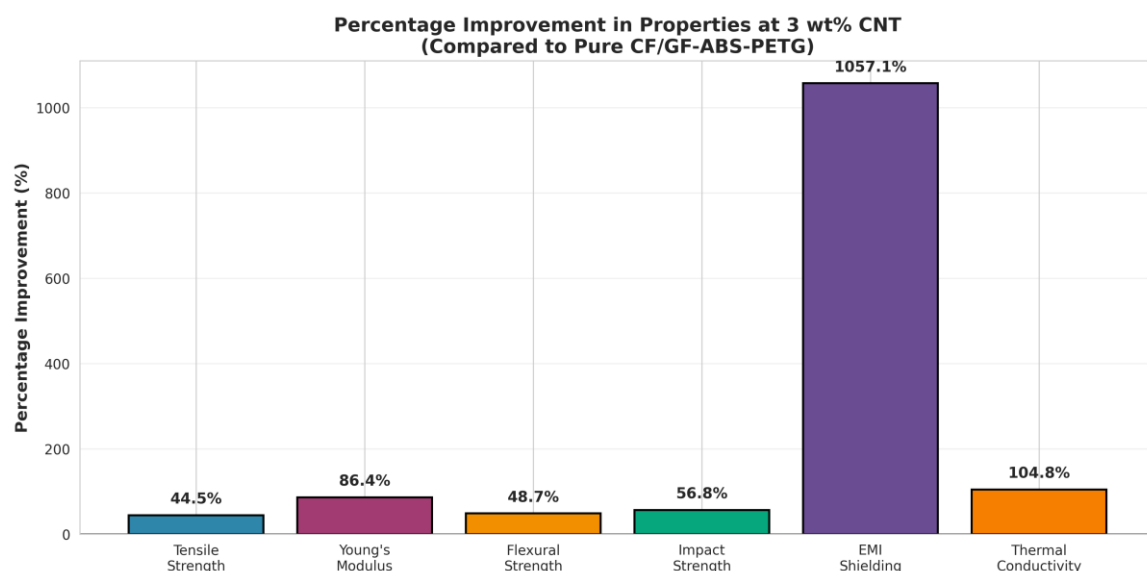


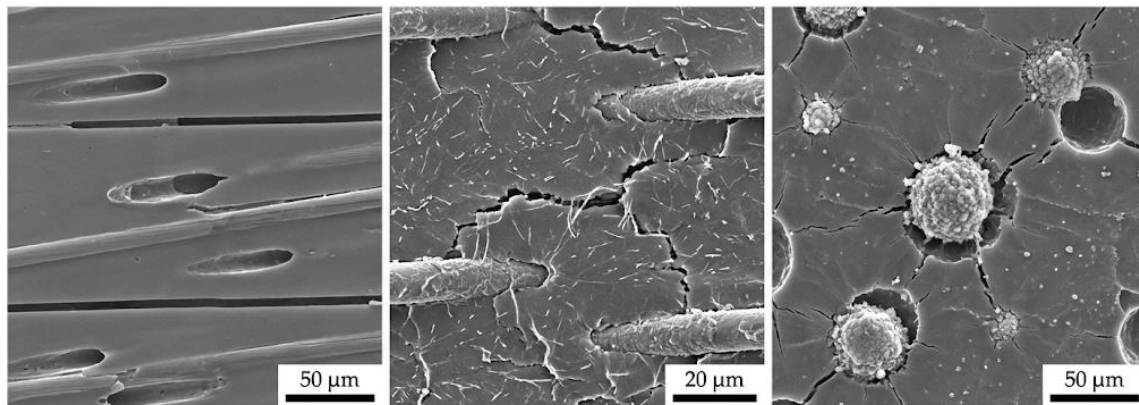
Figure 3: Percentage improvement in properties at 3 wt% CNT compared to pure CF/GF-ABS-PETG composite.

Figure 3 presents percentage improvements at optimal 3 wt% MWCNT loading across all properties. The dramatic Young's modulus improvement (+86.4%) combined with substantial strength enhancements demonstrates effective load transfer from matrix to MWCNT reinforcement. Thermal conductivity improvement (+104.8%) at 3 wt% confirms percolation network formation while maintaining mechanical property balance.

3.4. Microstructural analysis

SEM imaging revealed critical insights into MWCNT distribution and fracture mechanisms. Baseline composites (0 wt% MWCNT) exhibited smooth matrix regions with fiber pull-out voids (20-40 μm lengths), indicating weak fiber-matrix bonding. Inter-layer gaps (5-15 μm) represented primary failure sites characteristic of FDM processing layer-by-layer deposition.

At optimal loading (3 wt%), uniform MWCNT dispersion was observed as individual nanotubes and small bundles (2-5 nanotubes). MWCNTs bridged inter-layer gaps, enhancing inter-layer adhesion. Fiber surfaces exhibited thin MWCNT-enriched polymer layers, improving interfacial bonding through mechanical interlocking and increased contact area. Fracture surfaces displayed increased roughness, indicating enhanced energy dissipation during failure through multiple crack deflection paths.



(a) 0 wt% MWCNT: smooth matrix with fiber pull-out voids (20-40 μm) and inter-layer gaps (5-15 μm). (b) 3 wt% MWCNT: uniform nanotube dispersion, inter-layer bridging, and rough fracture surface indicating enhanced energy dissipation. (c) 5 wt% MWCNT: large agglomerates (10-50 μm) with debonded voids (20-80 μm) acting as crack initiation sites.

Figure 4 presents SEM fracture surfaces of FDM-printed fiber-reinforced composites: (a) 0 wt% MWCNT showing smooth matrix, fiber pull-out voids and inter-layer gaps: (b) 3 wt% MWCNT with uniform MWCNT dispersion, nanotube bridging across layers, and rough fracture surfaces: (c) 5 wt% MWCNT exhibiting large MWCNT agglomerates with deboned voids and radial cracks, confirming agglomeration-controlled failure at high loading.

At high loading (5 wt%), MWCNT agglomerates (10-50 μm diameter) appeared as dense spherical clusters acting as crack initiation sites with radial crack patterns emanating from agglomerate periphery. Debonded agglomerates created large voids (20-80 μm), directly correlating with reduced tensile, flexural, and impact properties despite continued stiffness enhancement. This confirms agglomeration as the primary mechanism limiting mechanical performance at MWCNT loadings exceeding 3 wt%. Shown in figure.4

3.5. Reinforcement mechanisms

Mechanical property enhancement arises from hierarchical reinforcement mechanisms operating at multiple length scales:

1. **Load transfer:** High aspect ratio MWCNTs (length/diameter \sim 1000-1500) enable efficient stress transfer through interfacial shear stress. The large interfacial area provides extensive matrix-nanotube contact for load distribution.
2. **Crack deflection:** MWCNTs deflect propagating cracks along their length, forcing longer tortuous paths and increasing fracture energy. Each deflection event dissipates energy through plastic deformation of surrounding matrix.
3. **Nano-bridging:** Individual MWCNTs bridge micro-cracks, providing closure stress resisting crack propagation. This mechanism is particularly effective for impact and fracture toughness enhancement.
4. **Enhanced interfacial bonding:** MWCNTs concentrate at fiber-matrix interfaces, creating nano-reinforced interphase regions with enhanced shear strength. This improves load transfer from matrix to macroscale fiber reinforcement.
5. **Void reduction:** MWCNT networks bridge inter-layer voids characteristic of FDM processing, improving material continuity and reducing stress concentration sites.

Agglomeration at loadings exceeding 3 wt% creates stress concentration sites with amplification factors of 2-3, reduces effective interfacial area by 60-80%, and renders 50-70% of MWCNTs ineffective within agglomerate interiors where load transfer cannot occur.

3.6. Comparison with literature

Table 4 compares the present results with literature values for FDM-printed CNT and fiber-reinforced composites. The hybrid CF/GF/MWCNT system demonstrates superior performance versus MWCNT-only reinforcement systems, confirming synergistic effects of combining macroscale fiber with nanoscale reinforcement. Performance approaches continuous fiber-reinforced systems (tensile strength 61.4 MPa vs. 59.3 MPa for CF-PLA) despite using short fibers, attributed to MWCNT-mediated interfacial enhancement bridging the performance gap.

Table 4: Comparison with literature values for FDM-printed CNT and fiber-reinforced composites

Material System	σ_t (MPa)	E (GPa)	σ_f (MPa)
CF/GF-ABS-PETG + 3% MWCNT (This study)	61.4	4.12	101.7
ABS + 3% MWCNT [16]	38.5	2.85	58.2
ABS + 1% MWCNT [18]	41.2	2.65	--
CF-PLA (100% infill) [9]	59.3	--	--
CF-PLA (continuous fiber) [7]	112.5	6.85	187.3
Pure ABS (FDM) [19]	35.2	2.08	52.1

3.7. Application potential

The characterized mechanical-thermal property combinations position MWCNT-enhanced CF/GF-ABS-PETG composites for multiple engineering applications. For aerospace applications, the high strength-to-weight ratio (specific strength ~ 57 kN·m/kg at 3 wt%) and enhanced thermal stability ($T_g = 110.3^\circ\text{C}$) are suitable for interior brackets, instrument housings, and non-structural fairings. The complex geometry capability from FDM enables integrated features unachievable through conventional manufacturing.

For marine applications, tensile strength (61.4 MPa) and flexural strength (101.7 MPa) at 3 wt% MWCNT are sufficient for lightweight deck fittings, autonomous underwater vehicle (AUV) components, and electronics housings. The corrosion resistance of polymer matrix eliminates galvanic corrosion concerns versus aluminum alloys. Enhanced thermal conductivity (0.385 W/m·K at 3 wt%) enables passive heat dissipation for electronics systems. However, marine deployment requires UV stabilization and surface barrier coatings for extended seawater exposure.

For structural applications, the balanced mechanical properties (strength, stiffness, and toughness simultaneously enhanced) combined with tailorable thermal conductivity enable load-bearing components requiring thermal management, such as robotics structures, tooling, and fixtures.

4. CONCLUSIONS

This study systematically investigated MWCNT loading effects (1-5 wt%) on mechanical and thermal properties of hybrid CF/GF-reinforced ABS-PETG composites fabricated via FDM. The following conclusions are drawn:

1. Optimal mechanical performance was achieved at 3 wt% MWCNT loading, providing balanced multifunctional properties: tensile strength increased 44.5% to 61.4 MPa, Young's modulus increased 86.4% to 4.12 GPa, flexural strength increased 48.7% to 101.7 MPa, and impact strength increased 56.8% to 19.6 kJ/m².
2. MWCNT loadings exceeding 3 wt% induced agglomeration creating stress concentration sites, reducing tensile, flexural, and impact properties despite continued stiffness enhancement, confirming dispersion quality as the critical factor governing mechanical performance.
3. Glass transition temperature increased progressively with MWCNT content, reaching 111.2°C at 5 wt% (+5.1°C), expanding service temperature range for demanding applications through polymer chain immobilization effects.

4. Thermal conductivity exhibited dramatic enhancement (+188% at 5 wt%), reaching 0.542 W/m·K, enabling thermal management applications with percolation threshold at approximately 1 wt% MWCNT.
5. TGA revealed complex degradation behavior with onset temperature decreasing 5.3% at 5 wt% due to catalytic effects of residual metal impurities, while maximum degradation temperature remained stable, indicating bulk decomposition mechanisms unaffected by MWCNT presence.
6. Hierarchical reinforcement combining macroscale CF/GF reinforcement and nanoscale MWCNT reinforcement produced synergistic effects exceeding individual contributions, with MWCNTs enhancing fiber-matrix interfacial bonding and reducing FDM inter-layer voids.
7. SEM analysis confirmed direct correlation between mechanical property maxima at 3 wt% and uniform MWCNT dispersion, while property degradation at 5 wt% correlated with agglomerate formation (10-50 μm diameter).
8. The multifunctional composite system demonstrates strong application potential for aerospace interior components, marine AUV structures, electronics housings, and structural applications requiring balanced mechanical-thermal properties and design flexibility from additive manufacturing.

Future work should focus on surface functionalization strategies to improve MWCNT dispersion at higher loadings, investigation of fatigue and creep behavior for structural qualification, and development of multi-material printing strategies to create functionally graded MWCNT distributions optimized for specific loading conditions.

ACKNOWLEDGMENTS

This research was conducted at the Department of Marine Engineering, Andhra University, Visakhapatnam. The authors gratefully acknowledge use of the Materials Characterization Facility for SEM, TGA-DSC, and mechanical testing equipment. Technical support from Mr. K. Ravi Kumar for FDM printing assistance is acknowledged.

Data availability

The raw data supporting the findings of this study are available from the corresponding author upon reasonable request.

Declaration of competing interest

The authors declare that they have no known competing financial interests or personal relationships that could have appeared to influence the work reported in this paper.

REFERENCES

- [1] Gibson I, Rosen D, Stucker B, Khorasani M. Additive manufacturing technologies. 3rd ed. Springer; 2021.
- [2] Ngo TD, Kashani A, Imbalzano G, Nguyen KT, Hui D. Additive manufacturing (3D printing): A review of materials, methods, applications and challenges. *Compos Part B Eng* 2018;143:172-96.
- [3] Jamal MA, et al. Additive manufacturing of continuous fiber-reinforced polymer composites via fused deposition modelling: A comprehensive review. *Polymers* 2024;16(12):1622.
- [4] Ismail KI, Yap TC, Ahmed R. 3D-printed fiber-reinforced polymer composites by fused deposition modelling: Current status and future perspective. *Polymers* 2022;14(21):4659.
- [5] Rajpurohit SR, Dave HK. Analysis of tensile strength of a fused filament fabricated PLA part using an open-source 3D printer. *Adv Manuf* 2019;7(3):371-80.
- [6] Khosravani MR, Berto F, Ayatollahi MR, Reinicke T. Characterization of 3D-printed PLA parts with different raster orientations and printing speeds. *Sci Rep* 2022;12:1016.
- [7] Heidari-Rarani M, Rafiee-Afarani M, Zahedi AM. Mechanical characterization of FDM 3D printing of continuous carbon fiber reinforced PLA composites. *Compos Part B Eng* 2019;175:107147.
- [8] Tian X, Liu T, Yang C, Wang Q, Li D. Interface and performance of 3D printed continuous carbon fiber reinforced PLA composites. *Compos Part A Appl Sci Manuf* 2016;88:198-205.
- [9] Liu Z, Lei Q, Xing S. Mechanical characteristics of wood, ceramic, metal and carbon fiber-based PLA composites fabricated by FDM. *J Mater Res Technol* 2019;8(5):3741-51.
- [10] Bochnia J, Blasiak M, Koziar T. A comparative study of the mechanical properties of FDM 3D prints made of PLA and carbon fiber-reinforced PLA for thin-walled applications. *Materials* 2021;14(22):7062.
- [11] Yu MF, Lourie O, Dyer MJ, Moloni K, Kelly TF, Ruoff RS. Strength and breaking mechanism of multiwalled carbon nanotubes under tensile load. *Science* 2000;287(5453):637-40.
- [12] Thostenson ET, Ren Z, Chou TW. Advances in the science and technology of carbon nanotubes and their composites: A review. *Compos Sci Technol* 2001;61(13):1899-1912.
- [13] Coleman JN, Khan U, Blau WJ, Gun'ko YK. Small but strong: A review of the mechanical properties of carbon nanotube-polymer composites. *Carbon* 2006;44(9):1624-52.

- [14] Ma PC, Siddiqui NA, Marom G, Kim JK. Dispersion and functionalization of carbon nanotubes for polymer-based nanocomposites: A review. *Compos Part A Appl Sci Manuf* 2010;41(10):1345-67.
- [15] Spitalsky Z, Tasis D, Papagelis K, Galiotis C. Carbon nanotube-polymer composites: Chemistry, processing, mechanical and electrical properties. *Prog Polym Sci* 2010;35(3):357-401.
- [16] Singh P, Singari RM, Mishra RS. Enhanced mechanical and thermal properties of MWCNT-reinforced ABS nanocomposites prepared by twin-screw extrusion for fused filament fabrication. *Polym Adv Technol* 2024;35:e6308.
- [17] Sezer HK, Eren O. FDM 3D printing of MWCNT reinforced ABS nano-composite parts with enhanced mechanical and electrical properties. *J Manuf Process* 2019;37:339-47.
- [18] Gangadhar TG, Kumar SS, Devi GR, Rao PS. Mechanical performance of ABS/CNT nanocomposites developed by fused deposition modelling. *Mater Technol* 2025;40(7):2451862.
- [19] Ziemian S, Okwara M, Ziemian CW. Tensile and fatigue behavior of layered acrylonitrile butadiene styrene. *Rapid Prototyp J* 2015;21(3):270-8.
- [20] Domingo-Espin M, Borros S, Agullo N, Garcia-Granada AA, Reyes G. Influence of building parameters on the dynamic mechanical properties of polycarbonate fused deposition modeling parts. *3D Print Addit Manuf* 2014;1(2):70-7.
- [21] Petousis M, Vidakis N, Mountakis N, Karapidakis E, Moutsopoulou A. Functionality versus sustainability for PLA in MEX 3D printing: The impact of generic process control factors on flexural response and energy efficiency. *Polymers* 2023;15(5):1232.
- [22] Moradi M, Meiabadi MS, Kaplan A. 3D printed parts with honeycomb internal pattern by fused deposition modelling; experimental characterization and production optimization. *Met Mater Int* 2019;25:1312-25.